

OMAE2003-37022

ON SECOND-ORDER ROLL MOTIONS OF SHIPS

YONGHUI LIU (ALLEN)

FMC SOFEC FLOATING SYSTEM, INC.
6677 N. GESSNER, HOUSTON, TX 77040, USA
Email: allen.liu@fmcti.com

Keywords: Roll motions, second-order roll motions, Ships, difference-frequency wave forces, HOBEM.

ABSTRACT

More and more vessels for offshore engineering applications have a roll period beyond 20 seconds in order to avoid the wave frequency excitations on the roll motion. That is particularly true for the latest drilling vessels. However, this will lead to an unexpected second-order roll motion of the ships. This paper will present a new methodology to evaluate the second-order roll motions of the ships in random seas. The higher-order boundary element method (HOBEM) has been utilized to generate the second order difference-frequency roll excitations on the ships and the second-order ship roll motions were predicted by a frequency-domain method. A series of model tests have been conducted and the test results have a good agreement with the numerical predictions. Therefore, this new method has been verified and validated.

INTRODUCTION

Most of the ships have a roll period within the range of the wave periods. Thus, their roll motions can be evaluated accurately by the linear wave theory. However, the latest drilling ships and some specially designed floating production storage offloading tankers (FPSO) have a roll natural period away from the wave-frequency zone in order to avoid the unacceptably large wave induced roll motions. The normal practices are to increase the roll period beyond 20 seconds, which are away from the typical wave period zone of 5 to 20 seconds. As a results, the second-order difference-frequency

wave loads occurring close to the natural frequency of the ship roll motions often give greater contributions to the low-frequency resonant roll response. In order to predict those roll resonant response in a reliable manner, designers need to compute the second-order different-frequency wave loads on the ship roll motions.

There are extensive researches have been conducted on the wave-frequency roll motions of ships. A lots of results and techniques on the ship roll motions can be found in the text books and papers, for instance, [1-3]. However, only limited information is available to the second-order difference-frequency roll motions of the ships primarily due to the difficulty associated with the evaluations of the second-order wave excitations on roll motions. The other reason might be that it was simply overlooked.

The higher-order boundary element method (HOBEM) has been developed in [4,5] by Liu et al to evaluate the linear wave loads on three-dimensional bodies and later extended to the non-linear second-order sum- and difference-frequency wave forces [6-9].

This paper presents a new method to evaluate the second-order difference-frequency roll motions of a ship in frequency domain. The first- and second-order wave roll excitations were computed by HOBEM and utilized to calculate the first- and second-order ship roll motions. A series of model tests with FPSO tankers have been conducted. The model test results have been utilized to compare with the numerical predictions. An excellent agreement between the model test and numerical results has verified and validated this new method.

$\Omega^{(i)}=(\Omega_1^{(i)}, \Omega_2^{(i)}, \Omega_3^{(i)})$, ($i=1,2$) denotes i -th order translational and rotational motions, respectively.

FIRST- AND SECOND-ORDER WAVE FORCES

We consider the first- and second-order interaction of plane bichromatic incident waves with three-dimensional bodies. For analysis, Cartesian coordinates with the xy -plane in the quiescent free surface and z positive upward are used. Assuming the ideal fluid and weak non-linearities, we express the total velocity potential Φ as a sum of first- and second-order potentials:

$$\Phi = \varepsilon \Phi^{(1)} + \varepsilon^2 \Phi^{(2)} \quad (1)$$

At each order, the velocity potentials are decomposed into incident, diffraction and radiation potentials:

$$\Phi^{(i)} = \Phi_I^{(i)} + \Phi_D^{(i)} + \Phi_R^{(i)}, i=1,2 \quad (2)$$

In the presence of bichromatic incident waves with frequencies ω_1 and ω_2 , we can write the velocity potential Φ and force \mathbf{F} in the form:

$$\begin{aligned} \begin{pmatrix} \Phi(x,t) \\ \mathbf{F}(t) \end{pmatrix} &= \varepsilon \sum_{j=1}^2 \operatorname{Re} \left(\begin{pmatrix} \Phi_j^{(1)}(x) \\ \mathbf{f}_j^{(1)} \end{pmatrix} e^{-i\omega_j t} \right) + \varepsilon^2 \sum_{j=1}^2 \sum_{k=1}^2 \\ &\operatorname{Re} \left(\begin{pmatrix} \Phi_{jk}^{(d)}(x) \\ \mathbf{f}_{jk}^{(d)} \end{pmatrix} e^{-i(\omega_j - \omega_k)t} + \begin{pmatrix} \Phi_{jk}^{(s)}(x) \\ \mathbf{f}_{jk}^{(s)} \end{pmatrix} e^{-i(\omega_j + \omega_k)t} \right) \end{aligned} \quad (3)$$

The superscriptions of (d) and (s) denotes the second-order difference- and sum-frequency components. The first- and second-order wave forces are given respectively by

$$\mathbf{F}^{(1)} = -\rho \iint_{S_B} \frac{\partial \Phi^{(1)}}{\partial t} \mathbf{n} dS - \rho g A_w (\Psi_3^{(1)} + y_f \Omega_1^{(1)} - x_f \Omega_2^{(1)}) \mathbf{k} \quad (4a)$$

$$\begin{aligned} \mathbf{F}^{(2)} &= -\rho \iint_{S_B} \frac{\partial \Phi^{(2)}}{\partial t} \mathbf{n} dS - \rho g A_w (\Psi_3^{(2)} + y_f \Omega_1^{(2)} - x_f \Omega_2^{(2)}) \mathbf{k} \\ &+ \frac{\rho g}{2} \oint_{WL} (\zeta_r^{(1)})^2 \mathbf{N} dl - \rho \iint_{S_B} \left(\frac{1}{2} \nabla \Phi^{(1)} \cdot \nabla \Phi^{(1)} + (\Psi^{(1)} + \Omega^{(1)} \times \mathbf{x}) \cdot \frac{\partial}{\partial t} \nabla \Phi^{(1)} \right) \mathbf{n} dS \\ &+ \Omega^{(1)} \times \mathbf{F}^{(1)} - \rho g A_w (y_f \Omega_2^{(1)} \Omega_3^{(1)} + x_f \Omega_1^{(1)} \Omega_3^{(1)}) \mathbf{k} \end{aligned} \quad (4b)$$

where ρ is the fluid density, A_w the water plane area, S_B the mean body surface, WL the waterline, (x_f, y_f) the center of floatation of A_w , \mathbf{x} the position vector, $\mathbf{n}=(n_1, n_2, n_3)$ the unit normal vector, and \mathbf{k} the unit vector in the z -axis, $\mathbf{N}=\mathbf{n}/(1-n_3^2)^{1/2}$. The first-order relative wave height is defined as $\zeta_r^{(1)}=\zeta^{(1)}-\Psi^{(1)}-y\Omega_1^{(1)}+x\Omega_2^{(1)}$. $\Psi^{(i)}=(\Psi_1^{(i)}, \Psi_2^{(i)}, \Psi_3^{(i)})$ and

The corresponding expressions for the first- and second-order moments are given by, see Ogilvie [10] (1983) or Liu et al [6] (1992).

$$\mathbf{M}^{(1)} = -\rho \iint_{S_B} (\mathbf{x} \times \mathbf{n}) \left[\frac{\partial \Phi^{(1)}}{\partial t} + g(\Psi_3^{(1)} + y\Omega_1^{(1)} - x\Omega_2^{(1)}) \right] dS \quad (5a)$$

$$\begin{aligned} \mathbf{M}^{(2)} &= -\rho \iint_{S_B} (\mathbf{x} \times \mathbf{n}) \left[\frac{\partial \Phi^{(2)}}{\partial t} + g(\Psi_3^{(2)} + y\Omega_1^{(2)} - x\Omega_2^{(2)}) \right] dS \\ &+ \frac{\rho g}{2} \oint_{WL} (\zeta_r^{(1)})^2 (\mathbf{x} \times \mathbf{N}) dl - \rho \iint_{S_B} (\mathbf{x} \times \mathbf{n}) \left(\frac{1}{2} \nabla \Phi^{(1)} \cdot \nabla \Phi^{(1)} + (\Psi^{(1)} + \Omega^{(1)} \times \mathbf{x}) \cdot \frac{\partial}{\partial t} \nabla \Phi^{(1)} \right) dS \\ &+ \Psi^{(1)} \times \mathbf{F}^{(1)} + \Omega^{(1)} \times \mathbf{M}^{(1)} \\ &- \rho g (\Omega_1^{(1)} \Omega_3^{(1)} J_{12} + \Omega_2^{(1)} \Omega_3^{(1)} J_{22} + \Omega_2^{(1)} \Omega_3^{(1)} z_b \nabla + \frac{1}{2} (\Omega_1^{(1)^2} + 2\Omega_2^{(1)^2} + \Omega_3^{(1)^2}) y_b \nabla) \mathbf{i} \\ &+ \rho g (\Omega_2^{(1)} \Omega_3^{(1)} J_{12} + \Omega_1^{(1)} \Omega_3^{(1)} J_{11} + \Omega_1^{(1)} \Omega_3^{(1)} z_b \nabla + \Omega_1^{(1)} \Omega_2^{(1)} y_b \nabla + \frac{1}{2} (2\Omega_1^{(1)^2} + \Omega_2^{(1)^2} + \Omega_3^{(1)^2}) x_b \nabla) \mathbf{j} \end{aligned} \quad (5b)$$

where ∇ is the displacement of the body, and x_b, y_b and z_b are the coordinates of the center of buoyancy. In addition, $(\mathbf{i}, \mathbf{j}, \mathbf{k})$ are unit vectors of x, y and z axes, and $J_{ik} = \iint_{WP} x_i x_k dS$ denotes the moments of the water plane area.

The Eqs. (4b) and (5b) also provide the added mass, wave damping and hydrodynamic coefficients for the second-order motions at sum- and difference-frequency, and the procedure is identical to that of the first-order radiation problem except for the shift of relevant frequency. The time mean components of the Eqs. (3), (4b) and (5b) were extensively studied by Liu et al [7] (1992). In this paper, particular attention is paid on the second-order difference-frequency forces and moments.

Since the contributions from the second-order velocity potential $\Phi^{(2)}$ to the total difference-frequency wave forces and moments are less important than the other components represented by the quadratic products of the first-order quantities, see for example [11], the quadratic transfer functions of the second-order difference-frequency wave excitations will be approximated by excluding the second-order velocity potential $\Phi^{(2)}$.

HIGHER-ORDER BOUNDARY ELEMENT METHOD

In this section, we briefly describe the higher-order boundary element method (HOBEM). For simplicity, we use the notation ϕ here to represent either $\phi_D^{(i)}$ or $\phi_R^{(i)}$. Only the first-order wave-frequency problem will be discussed here.

The use of Green's theorem with ϕ and the free-surface Green function G leads to the following integral equation:

$$c(\mathbf{p})\phi(\mathbf{p}) = \frac{1}{4\pi} \iint_{S_B} [G(\mathbf{p}, \mathbf{q}) \frac{\partial \phi(\mathbf{q})}{\partial n_q} - \phi(\mathbf{q}) \frac{\partial G(\mathbf{p}, \mathbf{q})}{\partial n_q}] dS \quad (6)$$

where \mathbf{p} and \mathbf{q} represent field and source point vectors, respectively, and $c(\mathbf{p})$ is a normalized solid angle at point \mathbf{p} on the boundary surface S_B . Employing higher-order isoparametric elements, the body surface, velocity potential and its normal derivatives can be expressed by the higher-order shape functions on each element:

$$[x, y, z] = \sum_{j=1}^s N_j(\xi, \eta) [x_j, y_j, z_j] \quad (7)$$

$$\phi(\mathbf{q}) = \sum_{j=1}^s N_j(\xi, \eta) \phi_j, \quad \frac{\partial \phi(\mathbf{q})}{\partial n_q} = \sum_{j=1}^s N_j(\xi, \eta) \left(\frac{\partial \phi}{\partial n} \right)_j \quad (8)$$

where ϕ_j and $\left(\frac{\partial \phi}{\partial n} \right)_j$ are the values at the j -th node and s denotes the number of the nodes on each element. For instance, the shape function for a quadrilateral quadratic element with 8-nodes can be expressed as (Zienkiewicz [12], 1977):

$$N_j(\xi, \eta) = \begin{cases} \frac{1}{4}(1 + \xi_j \xi)(1 + \eta_j \eta)(-1 + \xi_j \xi + \eta_j \eta) & j = 1, 3, 5, 7 \\ \frac{1}{2}(1 + \xi_j \xi + \eta_j \eta)[1 - (\eta_j \xi)^2 - (\xi_j \eta)^2] & j = 2, 4, 6, 8 \end{cases} \quad (9)$$

Upon discretizing the body surface S_B with M higher-order elements and substituting Eqs. (8) and (9) in to Eq. (6), we obtain the following algebraic equation for the unknown ϕ_k :

$$\sum_{j=1}^{NOD} H_{ik} \phi_k = \sum_{j=1}^{NOD} D_{ik} \left(\frac{\partial \phi}{\partial n} \right)_k \quad i = 1, 2, \dots, NOD \quad (10)$$

where,

$$H_{ik} = \sum_{e=1}^M \sum_{j=1}^s \delta_{kr} \hat{H}_{ij}^{(e)} + c_i \delta_{ik} \quad (11)$$

$$D_{ik} = \sum_{e=1}^M \sum_{j=1}^s \delta_{kr} \hat{D}_{ij}^{(e)} \quad (12)$$

and NOD is the total number of nodes on the body surface S_B . In Eqs. (11) and (12), δ_{kr} denotes Kronecker delta and $r = NENN(j, e)$ is a connective matrix, which represents the correspondence between the local and global nodes.

The functions $\hat{H}_{ij}^{(e)}$ and $\hat{D}_{ij}^{(e)}$ are given by:

$$\hat{H}_{ij}^{(e)} = \frac{1}{4\pi} \iint_{\Gamma_e} \frac{\partial G(\mathbf{p}, \mathbf{q})}{\partial n_q} N_j d\Gamma_q \quad (13)$$

$$\hat{D}_{ij}^{(e)} = \frac{1}{4\pi} \iint_{\Gamma_e} G(\mathbf{p}, \mathbf{q}) N_j d\Gamma_q \quad (14)$$

where N_j is the j -th shape function and Γ_e the surface of each element. The full descriptions about the HOBEM can be found in Liu, et al [4-8].

SECOND-ORDER ROLL MOTIONS OF SHIPS

The first-order wave-frequency, second-order mean and difference-frequency roll moments on the vessel are evaluated by the above advanced hydrodynamic theory and HOBEM. The equation of the ship roll motion of a linearized system exposed to random seas can be written as:

$$M_{44} \ddot{\Omega}_1 + C_{44} \dot{\Omega}_1 + K_{44} \Omega_1 = M_x^{(1)}(t) + M_x^{(2)}(t) \quad (15)$$

where K_{44} is a linear restoring coefficient for roll motion; $M_{44} = m_{44} + a_{44}$, m_{44} is roll mass inertia and a_{44} roll added mass coefficient, C_{44} an equivalent roll damping coefficient. $M_x^{(1)}(t)$ and $M_x^{(2)}(t)$ are the first-order wave-frequency and second-order difference-frequency roll moments on the ship.

In the frequency domain, the transfer functions and response of ship roll motions are evaluated based on the standard procedures of spectra analysis. The standard deviation of the roll motion will be given by

$$\sigma_{roll}^2 = \int_0^\infty \frac{S_{m_x}(\omega)}{(K_{44} - M_{44}\omega^2)^2 + C_{44}^2\omega^2} d\omega \quad (16)$$

where the spectra density of the roll moments, $S_{m_x}(\omega)$ can be written as the sum of the first-order wave-frequency and second-order difference-frequency components, $S_{m_x}^{(1)}(\omega)$ and $S_{m_x}^{(2)}(\mu)$, respectively. The μ is the difference-frequency between $\omega_i (= \omega)$ and $\omega_j (= \omega + \mu)$

$$S_{m_x}^{(1)}(\omega) = S_w(\omega) [M_x^{(1)}(\omega)]^2 \quad (17)$$

$$S_{m_x}^{(2)}(\mu) = 8 \int_0^\infty S_w(\omega) S_w(\omega + \mu) M_x^{(2)}(\omega) M_x^{(2)}(\omega + \mu) d\omega \quad (18)$$

where S_w is wave spectral density; $M_x^{(1)}$ and $M_x^{(2)}$ are the first-order wave-frequency linear and second-order difference-frequency quadratic roll moment transfer functions. Thus, we

can derive the stand deviations of the ship roll motions at wave- and low-frequency, $\sigma_{roll}^{(1)}$ and $\sigma_{roll}^{(2)}$, respectively.

With the assumption that the roll response of the ships is a narrow banded Gaussian process with Rayleigh distributed peaks, the most probable extreme values of the wave-frequency and low-frequency roll responses can be given by the product of the standard deviations and a peak factor [13]:

$$A = \sqrt{2 \ln N} \quad (19)$$

where N is either the total number of the wave-frequency roll cycles or the total number of the low-frequency cycles in a specified storm period. The maximum total roll motion is then approximately evaluated by

$$\Omega_1 = \Omega_1^{mean} + \Omega_1^{WF} + \Omega_1^{LF} \quad (20)$$

where mean, WF and LF denote the mean, wave- and low-frequency components of the ship roll motion.

NUMERICAL AND MODEL TEST RESULTS

The first- and second-order wave excitations on a 50,000 DWT tanker in deep water were evaluated by HOBEM and its first- and second-order roll motions were predicted by the formula presented in the preceding sections. The HOBEM model of the tanker was discretized with fifty-eight elements. This tanker has a roll period of 23.3 seconds, which is away from the wave-frequency zone. A series of model tests were carried out for the vessel at MARINTEK in Norway. The roll response transfer function and spectrum are represented in Figs. 1 and 2 with the associated wave spectrum. It clearly indicated that there is little wave energy around the roll natural period of 23.3 seconds. The model test results are listed in Table 1 and compared with the current predictions. An excellent agreement between the numerical results and measurements is observed. The dominant contribution to the total roll motions is coming from the second-order difference-frequency roll motions. It's very important to point that the second-order lower-frequency roll responses are usually governing the total roll response due to the small roll damping and little wave excitations around the roll natural periods. Therefore, the second-order ship roll motions should be evaluated for ships with long roll natural periods in order to ensure that any significant contributions from the second-order roll response are included in the final results. The second-order difference-frequency roll moment spectra density is shown in Fig. 3 with the roll response curves. As indicated, the roll moment spectra density at the roll natural period is significantly different from that at zero frequency. This means that the mean roll moment cannot be utilized to approximate the second-order roll moment spectra density. The complete quadratic roll moment transfer functions at difference-frequencies should be generated to compute the second-order ship roll motions.

The second-order roll motions analysis and model tests have also been carried out for a 170,000 new built FPSO tanker in shallow water. A total of seventy-three HOBEM elements

were utilized to model this tanker at its full draft. This tanker has the roll periods of 25.2 and 23.7 seconds for the fully loaded and ballast conditions, respectively. Both beam sea and quartering sea conditions have been analyzed and tested. The numerical results and model test data are presented in Table 2. The spectra densities of the second-order roll moments are represented in Fig. 4. Clearly, that the density at the roll periods are much bigger than those at the zero frequency. Therefore, it cannot be approximated by the mean roll moments only. The second-order roll motions dominant the total roll responses as expected. The numerical results and model test data are very close to each other.

CONCLUSIONS

The numerical model has been set up to compute the second-order ship roll motions in irregular waves in frequency-domain with satisfactory accuracy. The numerical results have been compared with the series of the model test data. The excellent agreements between numerical predictions and the model test results have validated and verified our numerical methodology. Therefore, we can evaluate the second-order ship roll motions accurately by this method. The results presented in the paper has indicated that the second-order roll motions shall be evaluated for a ship with a long roll period away from wave-frequency zone, since it will be the dominant contributions to the total ship roll motions. This analysis also revealed that there could have an optimized natural roll period zone for a given vessel and environmental conditions so that the maximum total roll motions of the vessel is minimized.

REFERENCES

- [1] Haskind, M.D., 1946, The hydrodynamic theory of ship oscillations in rolling and pitching, *Prikl. Mat. Mekh*, **10**, pp.33-36.
- [2] Hoff, J.R. and Aarsnes, J.V., 1986, Motion of a three-dimensional body including the effect of viscous damping in regular and irregular waves, MARINTEK Report.
- [3] Liu, Y.Z. and Miao, G.P., 1987, Theory of Ship Motions in Waves, Shanghai Jiao Tong University Press.
- [4] Liu, Yonghui, 1988, Analysis of fluid-structure interaction by using higher-order boundary elements in potential problems and its application in coupling vibrations of bending and torsion of ships, PH. D. Dissertation, Shanghai Jiao Tong University, China.
- [5] Liu, Y. H., Kim, C.H. and Lu, X.S., 1991, Comparison of Higher Order Boundary Element and Constant Panel Method for Hydrodynamic Loading, *Int. J. Offshore and Polar Engineering*, **1**, n. 1, pp. 8-17
- [6] Liu, Y. H., Kim, C.H., Kim, M.H. and Boo, S.Y., 1992, Second-order Mean Drift Forces and Moments on ISSC Tension Leg Platform in uni- and multi-directional random Seas, *Proc. ISOPE'92*, Vol 1, pp.218-227.
- [7] Liu, Y. H., Kim, C.H. and Kim, M.H., 1993, The Computation of Mean Drift Forces and Wave Run-up by HOBEM, *Int. J. Offshore and Polar Engineering*, **3**, n.2, pp. 101-106

- [8] Liu, Y. H., Kim, C.H. and Kim, M.H., 1993, Double-frequency wave loads on a compliant TLP, Proc. of ISOPE'93 Vol 1, pp.334-340.
- [9] Kim, C.H. and Kim, M.H., Liu, Y. H. and Zhao, C.T. 1994, Time domain simulation of nonlinear response of a coupled TLP system, Int. J. Offshore and Polar Engineering, **4**, n. 4, pp. 284-291
- [10] Ogilvie, T.F., 1983, Second-order hydrodynamic effects on ocean platforms, Intl. Workshop Ship and Platform Motions, Berkeley.
- [11] Kim, Moo-Hyun and Yue, Dick K.P., 1990, The complete second-order diffraction solutions for an axisymmetric body, Part 2. Bichromatic incident waves and body motions, J. Fluid Mech., **211**, pp557-593.
- [12] Zienkiewicz, O.C., 1977, Finite Element Method, McGraw-Hill.
- [13] Ochi, M.K., 1973, On prediction of extreme values, J. Ship Research, **17**, pp.29-37.

Table 1 Roll Motions of a Fully Loaded 50,000 DWT Tanker in Deep Water

Model Test Results	Test No.	Vessel Heading (deg)	Roll Motion			
			Mean (deg)	Max (deg)	Min (deg)	St. dev. (deg)
	503	12.28	0.06	2.32	-2.45	0.63
	504	12.84	0.39	2.79	-2.21	0.60
	505	13.86	0.34	3.29	-2.42	0.61
	506	14.02	0.50	2.99	-2.15	0.62
	507	12.89	0.62	3.18	-2.15	0.64
	508	13.32	0.45	2.83	-2.38	0.64
	509	13.31	0.36	2.86	-2.19	0.62
	510	13.63	0.38	2.50	-2.13	0.59
	511	12.93	0.46	3.12	-1.92	0.58
Average		13.23	0.40	2.88	-2.22	0.61
Theory	WF	13.00		0.61	-0.61	0.16
	LF	13.00	0.43	2.43	-1.57	0.57
	Total	13.00	0.43	3.04	-2.18	0.59

Table 2a Roll Motions of a Fully Loaded 170,000 DWT Tanker in Shallow Water

Wave Heading deg		Roll Period sec	Roll Motions				
				Mean deg	Max deg	Min deg	St. dev. deg
90	Theory	25.7	WF	0.00	1.41	-1.41	0.38
			LF	-0.70	10.16	-12.16	3.20
			Total	-0.70	11.57	-13.57	3.22
	Test	25.2	Total	0.43	9.84	-11.44	2.37
135	Theory	25.7	WF	0.00	2.34	-2.34	0.63
			LF	-0.48	2.94	-3.91	0.98
			Total	-0.48	5.28	-6.25	1.17
	Test	25.2	Total	-0.79	3.39	-7.45	1.11
160	Theory	25.7	WF	0.00	1.41	-1.41	0.38
			LF	-0.14	1.84	-2.12	0.57
			Total	-0.14	3.25	-3.53	0.69
	Test	25.2	Total	-0.26	3.73	-3.72	0.78

Table 2b Roll Motions of a Ballast 170,000 DWT Tanker in Shallow Water

Wave Heading deg		Roll Period sec	Roll Motions				
				Mean deg	Max deg	Min deg	St. dev. deg
90	Theory	23.1	Wave	0.00	2.12	-2.12	0.57
			Low	-0.45	10.30	-11.20	3.07
			Total	-0.45	12.42	-13.32	3.12
	Test	23.7	Total	-0.32	11.03	-11.87	2.45
135	Theory	23.1	Wave	0.00	2.23	-2.23	0.60
			Low	-0.17	2.03	-2.87	0.77
			Total	-0.17	4.26	-5.10	0.98
	Test	23.7	Total	-0.18	5.42	-4.84	1.21
160	Theory	23.1	Wave	0.00	1.19	-1.19	0.32
			Low	-0.11	1.21	-1.43	0.38
			Total	-0.11	2.40	-2.62	0.50
	Test	23.7	Total	-0.06	2.78	-2.27	0.70

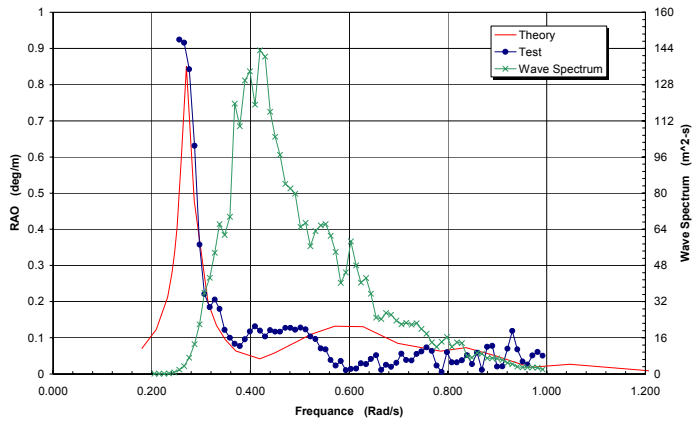


Figure 1 Roll Response Transfer Functions of 50,000 DWT Tanker

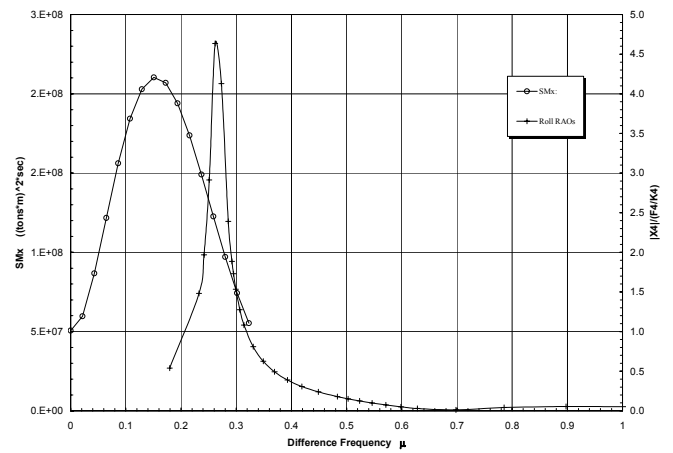


Figure 4 Roll Moment Spectra Density on 170,000 DWT Tanker in beam seas

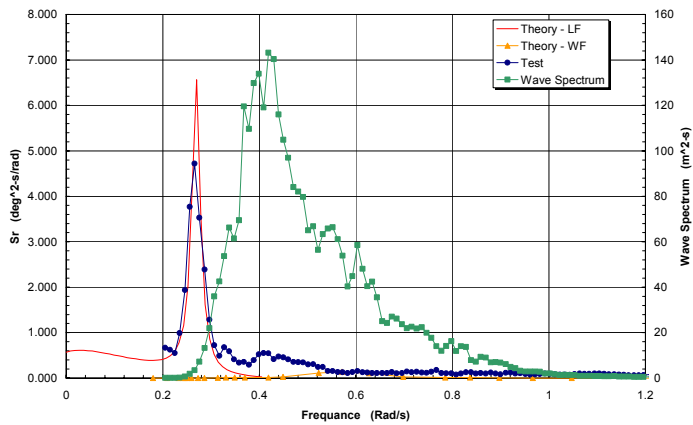


Figure 2 Roll Response Spectrum of 50,000 DWT Tanker

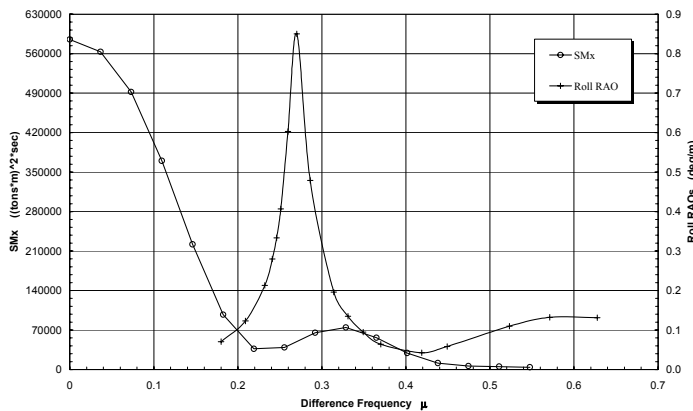


Figure 3 Low-Frequency Roll Moment Spectra Density on 50,000 DWT Tanker